



# Recommendation for reducing the crystalline lens exposure dose by reducing imaging field width in cone-beam computed tomography for image-guided radiation therapy: an anthropomorphic phantom study

Tatsuya Yoshida<sup>1,2</sup> · Koji Sasaki<sup>2</sup> · Tomoki Hayakawa<sup>1</sup> · Toshiyuki Kawadai<sup>1</sup> · Takako Shibasaki<sup>1</sup> · Yoshiyuki Kawasaki<sup>3</sup>

Received: 23 January 2024 / Revised: 23 March 2024 / Accepted: 26 April 2024 / Published online: 30 April 2024

© The Author(s), under exclusive licence to Japanese Society of Radiological Technology and Japan Society of Medical Physics 2024, corrected publication 2024

## Abstract

In cone-beam computed tomography (CBCT) for image-guided radiation therapy (IGRT) of the head, we evaluated the exposure dose reduction effect to the crystalline lens and position-matching accuracy by narrowing one side (X2) of the X-ray aperture (blade) in the X-direction. We defined the ocular surface dose of the head phantom as the crystalline lens exposure dose and measured using a radiophotoluminescence dosimeter (RPLD, GD-352 M) in the preset field (13.6 cm) and in each of the fields when blade X2 aperture was reduced in 0.5 cm increments from 10.0 to 5.0 cm. Auto-bone matching was performed on CBCT images acquired five times with blade X2 aperture set to 13.6 cm and 5.0 cm at each position when the head phantom was moved from  $-5.0$  to  $+5.0$  mm in 1.0 mm increment. The maximum reduction rate in the crystalline lens exposure dose was  $-38.7\%$  for the right lens and  $-13.2\%$  for the left lens when blade X2 aperture was 5.0 cm. The maximum difference in the amount of position correction between blade X2 aperture of 13.6 cm and 5.0 cm was 1 mm, and the accuracy of auto-bone matching was similar. In CBCT of the head, reduced blade X2 aperture is a useful technique for reducing the crystalline lens exposure dose while ensuring the accuracy of position matching.

**Keywords** Crystalline lens exposure dose · Image-guided radiation therapy (IGRT) · Cone-beam computed tomography (CBCT) · Blade · Position matching

## 1 Introduction

Exposure to the crystalline lens has been discussed, and to date, the threshold doses for developing cataracts are 1.5 Gy for acute exposure [1] and 8 Gy for chronic exposure [1];

however, ICRP Publ. 118 recommended a threshold dose of 0.5 Gy [2]. In contrast, Nakajima et al. [3] conducted an epidemiological study involving 730 atomic bomb survivors and reported that the threshold dose point estimates for cortical cataracts and posterior subcapsular opacity were 0.6 Sv and 0.7 Sv, respectively. However, because the lower 90% confidence limit was 0 Sv, the thresholds for cortical cataracts and posterior subcapsular opacities could not exceed 0 Sv. Further, Neriishi et al. [4] conducted an epidemiological study involving 3761 atomic bomb survivors (479 of whom underwent cataract surgery) who underwent biennial health examinations, and reported that the best dose threshold estimate was 0.1 Gy (95% confidence interval [CI]  $<0-0.8$  Gy) after adjusting for age, sex, diabetes mellitus, and other potential confounders. Based on these reports, trusting the cataract threshold dose of 0.5 Gy is dangerous,

---

Koji Sasaki, Tomoki Hayakawa, Toshiyuki Kawadai, Takako Shibasaki, Yoshiyuki Kawasaki are contributed equally to this work.

✉ Tatsuya Yoshida  
ssty900.9145@gmail.com

<sup>1</sup> Department of Radiology, Koritsu Tatebayashi Kosei General Hospital, Gunma, Japan

<sup>2</sup> Graduate School of Radiological Technology, Gunma Prefectural College of Health Sciences, Gunma, Japan

<sup>3</sup> Department of Radiology, Nippon Medical School Hospital, Tokyo, Japan

and the exposure dose of the crystalline lens should be reduced as much as possible.

In modern radiotherapy, the widespread use of high-precision radiotherapy, such as intensity modulated radiation therapy (IMRT) and stereotactic radiotherapy (SRT), can reduce the organ at risk (OAR) dose and create optimized dose distribution for the target [5–7]. In particular, treatment planning for radiotherapy of the head and the head and neck is planned to reduce the dose for the crystalline lens [8–10]. On the other hand, image-guided radiation therapy (IGRT) is important for the safe and accurate delivery of high-precision radiotherapy, but increased exposure dose has become a problem [11–13]. The American Association of Physicists in Medicine (AAPM) has a Task Group (TG) 180 report [14] that provides guidelines for the management of organ doses (absorbed doses) in each IGRT technique (two-dimensional and cone-beam computed tomography (CBCT) imaging with kV or MV X-rays). It also shows how to reduce the exposure dose in IGRT and recommends optimizing the imaging dose while ensuring the accuracy of position matching. Therefore, reducing the exposure dose for the crystalline lens during IGRT is important.

The gantry-mounted kV X-ray imaging system (On-Board Imager, OBI) in a Varian Medical Systems linear accelerator is equipped with an X-ray moving aperture (blade), which enables the acquisition of images with a reduced imaging field. Zhang et al. [15] recommended reducing the blade in the Y-direction for thoracic CBCT in children because non-thoracic organs are also exposed. Ding et al. [16] reported that reducing the blade in the Y-direction could reduce the exposure dose in pelvic CBCT. The blades are placed in pairs, X1 and X2 in the X-direction and Y1 and Y2 in the Y-direction, and each can be set asymmetrically. In head CBCT, the X-ray tube rotation angle is  $292 - 88^\circ$  counterclockwise (CCW), which can reduce the exposure dose reaching the crystalline lens compared to a trajectory passing in front of the head (e.g.,  $92 - 248^\circ$  CCW) (Fig. 1). However, at this angle, the X-ray is directly incident on the crystalline lens at the beginning of a scan. In such a case, the crystalline lens can be protected by reducing the lens side blade in the X-direction (hereinafter referred to as "X2").

This study aimed to evaluate the usefulness of reducing blade X2 aperture to reduce the exposure dose for the crystalline lens in head CBCT.

## 2 Methods

### 2.1 Geometric arrangement of measurements

To reproduce the head radiotherapy setup, a head phantom (THRA-1, Kyoto Kagaku, Kyoto, Japan) was placed on a baseplate (20CFHNSUB2, CIVCO, Orange City, Iowa,

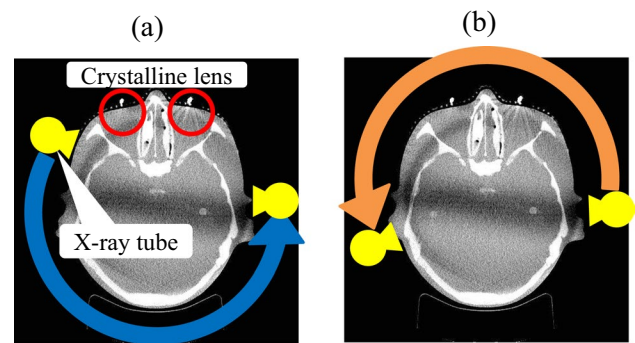


**Fig. 1** Relationship between the setting of X-ray tube rotation angle and crystalline lens position. **a** X-ray tube rotation angle of the posterior side to the head ( $292 - 92^\circ$ ), **b** X-ray tube rotation angle of the anterior side to the head ( $92 - 248^\circ$ ). In the definitions of both X-ray tube rotation angles, the X-ray tube angle of  $0^\circ$  equals the gantry angle of  $0^\circ$

USA) and pillow (MTSILVER2B, CIVCO Medical Solutions, Iowa, USA), with the radiophotoluminescence dosimeter (RPLD, GD-352 M, Chiyoda Technol, Tokyo, Japan) on the right and left eye surfaces of the head phantom (Fig. 2a) and fixed with a shell (MTAPUD2.4, CIVCO, Orange City, Iowa) (Fig. 2b). The dose measured by the RPLD in this geometric arrangement was defined as the “crystalline lens exposure dose.” The CBCT isocenter was set at the center of the head phantom in the left–right (X) and anterior–posterior (Z) directions and the superior–inferior (Y) direction at the eye position, which was defined as the reference position in the phantom coordinates in the IEC61217 [17] (Fig. 3).

### 2.2 Measurement of crystalline lens exposure dose in CBCT with reduced blade X2 aperture

A gantry-mounted kV X-ray imaging system (On-Board Imager: OBI, Varian Medical Systems, Palo Alto, USA) on a linear accelerator (Clinac iX, Varian Medical

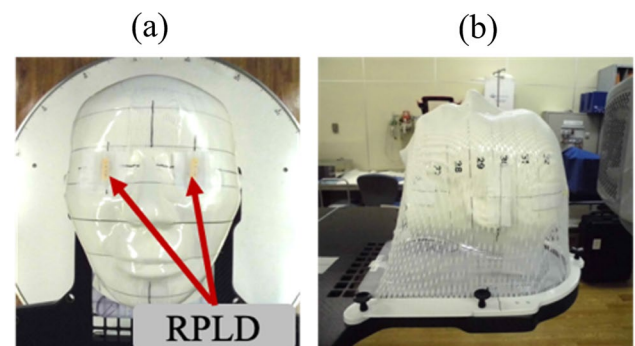


**Fig. 2** Photographs of geometric arrangements in crystalline lens exposure dose dosimetry. **a** RPLD placed on the surface of the eye, **b** head phantom fixed with a shell

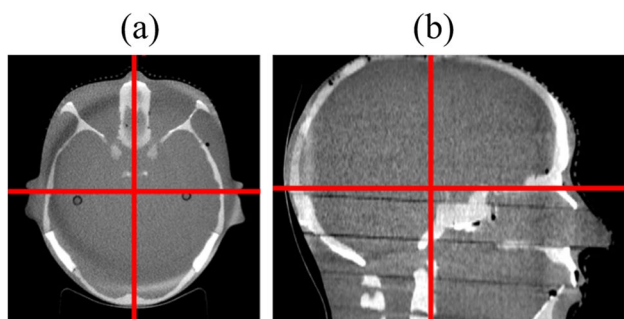
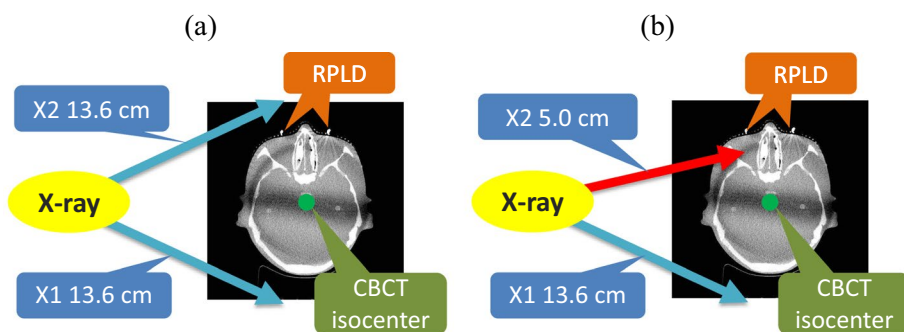


**Fig. 3** Reference position of the phantom coordinates in this study. The intersection of the crosshairs in the figures indicates the CBCT isocenter: **a** transverse plane, **b** sagittal plane

Systems, Palo Alto, USA) was used to measure the crystalline lens exposure dose. The CBCT imaging conditions were set to 100 kV, 145 mAs, an X-ray tube rotation angle of 292–88° (CCW), and a full-fan bowtie filter attachment (B300882R01C\_1252, Varian Medical Systems, Palo Alto, USA). The crystalline lens exposure dose was measured three times in each field when the blade aperture of the X-direction was reduced from the preset 27.2 cm (both X1 and X2 were 13.6 cm) to 5 cm for X2 only increments of 0.5 cm (Fig. 4 and 5).

**Fig. 4** Schematic diagram of imaging field X (imaging field width in anteroposterior direction). **a** Imaging field width of blades X1 and X2 on reference settings (blue arrow), **b** imaging field width of blade X2 changed to 5 cm (red arrow). The crystalline lens exposure dose was measured by changing field X2 from 10 to 5 cm in 0.5 cm increments



### 2.3 Calculation of absorbed dose and exposure dose reduction rates of crystalline lens

Before the crystalline lens exposure dose measurement, the RPLD was annealed and the background values were read using a glass dosimeter reader (FDG-1000, Chiyoda Technol, Tokyo, Japan). Measurement values were obtained by reading the amount of fluorescence with the glass dosimeter reader after a period of one week so that the fluorescence of radiophotoluminescence stabilized sufficiently because the RPLD was exposed to the CBCT scan.

The absorbed dose to the crystalline lens was calculated using the following formula:

$$D = (M - M_{BG}) \times \frac{\left(\frac{\mu_{en}}{\rho}\right)_{lens}}{\left(\frac{\mu_{en}}{\rho}\right)_{air}} \tag{1}$$

where D is the absorbed dose to the crystalline lens, M is the measured value,  $M_{BG}$  is the background value of fluorescence, and the unit for all is mGy.  $\left(\frac{\mu_{en}}{\rho}\right)_{lens}$  is the mass energy absorption coefficient of the crystalline lens, and  $\left(\frac{\mu_{en}}{\rho}\right)_{air}$  is the mass energy absorption coefficient of the air. The mass energy absorption coefficient was obtained from the Seltzer and Hubbell photon attenuation data [18]. In addition, Hsu and Kim [19, 20] reported that GD-352 M had good energy characteristics above 30 keV owing to the

kV Imager Positions (Varian IEC)			
TARGET		ACTUAL	
Gantry Rtn [deg]	22.0	Blade X1 [cm]	13.6
SAD [cm]	100.0	Blade X2 [cm]	5.0
IDU Vrt [cm]	50.0	Blade Y1 [cm]	9.1
IDU Lng [cm]	0.0	Blade Y2 [cm]	9.1
IDU Lat [cm]	0.0	Track Mode	On

**Fig. 5** Radiation therapy machine console display for changing blade X2 aperture (red frame). The setting value can be changed by entering the new value in the "TARGET" frame

improved energy dependence of the Sn filter. The energy dependence of GD-352 M was not considered because the effective energy was previously confirmed to be more than 30 keV when using a full-fan bowtie filter and because of the CBCT imaging conditions used in this study (100 kV, 145 mAs) [21].

To evaluate the crystalline lens exposure dose reduction effect based on the reduced X2 aperture, the crystalline lens exposure dose reduction rate was calculated using the following formula:

$$\varepsilon = \frac{D_{X2} - D_{ref}}{D_{ref}} \times 100 \quad (2)$$

where  $D_{ref}$  is the mean value of the absorbed dose to the crystalline lens when the blade X2 aperture is the preset value,  $D_{X2}$  is the mean value of the absorbed dose to the lens when the blade X2 aperture is reduced, and the unit for both is mGy.

#### 2.4 Measurement of distance between the CBCT isocenter and RPLD

The distance between CBCT isocenter and RPLD was measured to investigate the relationship between the X2 aperture and the effect of the crystalline lens exposure dose reduction (Fig. 6). First, a head phantom was imaged using a CT system (Emotion 16; Siemens Healthineers, Forchheim, Germany), and RPLDs and body were drawn on the surfaces of the right and left eyes on the CT images acquired

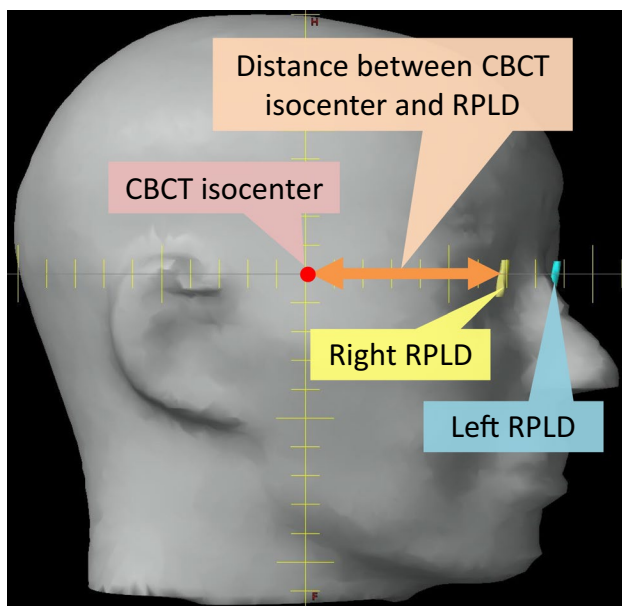


**Fig. 6** A method for measuring the distance between the CBCT isocenter and the RPLD using Beam's Eye View

using a treatment planning system (Eclipse Ver. 15.1, Varian Medical Systems, Palo Alto, USA). The isocenter of the treatment planning system was set as the CBCT isocenter in Sect. 2–1, and a 292°-X-ray tube angle field was created. The X-ray tube angle was changed from 292° in the CCW direction (that is, the direction of the X-ray tube rotation of CBCT), and the angle at which the RPLD was visible in Beam's Eye View was investigated. The angle at which the RPLD could be observed without overlapping the phantom body was defined as the “angle of primary X-ray incidence”.

#### 2.5 Evaluation of position matching accuracy in CBCT with reduced blade X2 aperture

An anatomy-matching software (Aria ver. 15.1, Varian Medical Systems, Palo Alto, USA) was used for position matching. The head phantom was moved in 1 mm increments from the reference position in the XYZ-direction from – 5 mm to + 5 mm on a ruler (SV-150KD, NIIGATA SEIKI CO., LTD., Niigata, Japan), and CBCT images were acquired five times at X2 aperture of 13.6 cm and 5.0 cm at all movement positions. Position matching was performed using an anatomy-matching software set such that the analysis range for auto-bone matching fully included the head, and the average value was calculated from the amount of position correction performed and recorded five times.

### 3 Results

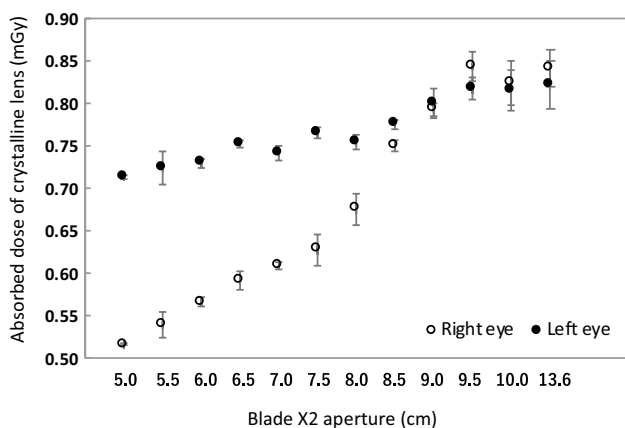
#### 3.1 Crystalline lens exposure dose with reduced blade X2 aperture

Figure 7 shows the crystalline lens exposure dose when X2 aperture is reduced. The left and right crystalline lens doses decreased at both X2 aperture of 13.6 cm and 8.5 cm; however, when X2 became smaller than 8.0 cm, the right crystalline lens dose decreased rapidly, and the left crystalline lens dose decreased slowly.

Table 1 shows a reduced reduction rate of the crystalline lens exposure dose with blade X2. The exposure dose reduction rate for the right crystalline lens was – 10.8% at X2 (8.5 cm) and – 25.4% at X2 (7.5 cm), with a rapid decrease in exposure dose between these two values and a maximum reduction rate of – 38.7% at X2 (5.0 cm). The reduction rate in the left crystalline lens exposure dose was more gradual than that in the right crystalline lens, and a maximum reduction rate of – 13.2% was observed at X2 aperture (5.0 cm).

#### 3.2 Distance between the CBCT isocenter and RPLD

Figure 8 shows the distance between CBCT isocenter and RPLDs at X-ray tube angles where the primary X-rays



**Fig. 7** Crystalline lens exposure dose when the imaging field of blade X2 aperture is changed. The ordinate depicts the absorbed dose of the crystalline lens (mGy) and the abscissa is the X2 aperture (cm). The white and black circles indicate the right and left crystalline lenses, respectively, and the error bars depict the standard deviation (SD) of the three measurements

incident on the RPLDs. The X-ray tube angles of primary X-ray incidence on the RPLD were 292–242° and 88° for the right RPLD and 292–267° and 118–88° for the left RPLD. The change in distance between CBCT isocenter and RPLD was 6.9–8.5 cm at 292–242° and 8.0 cm at 88° for the right RPLD and 7.8–8.7 cm at 292–267° and 8.4–8.7 cm at 118–88° for the left RPLD.

### 3.3 Position matching accuracy in CBCT with reduced blade X2

Table 2 shows the amount of position correction in auto-bone matching when X2 aperture was 13.6 cm and 5.0 cm. The difference in position correction between the X2 aperture of 13.6 cm and 5.0 cm was a maximum of 1 mm; however, the position matching accuracy was equivalent in most positions. Figure 9 shows a CBCT image with an X2 of 5.0 cm. Although artifacts were observed depending on the loss of the image area caused by the reduced X2 aperture, the CBCT isocenter and the structure on the left side of the head phantom were visible.

**Table 1** Reduction rate of exposure dose to the left and right crystalline lens by changing the aperture of the blade X2

Crystalline lens	Blade X2 apedrture(cm)											
	10.0	9.5	9.0	8.5	8.0	7.5	7.0	6.5	6.0	5.5	5.0	
Right	-2.1	0.2	-5.7	-10.8	-19.8	-25.4	-27.6	-29.7	-32.7	-35.9	-38.7	
Left	-0.8	-0.6	-2.7	-5.6	-8.2	-6.9	-9.8	-8.4	-11.2	-11.9	-13.2	

## 4 Discussion

In CBCT of the head, we evaluated the crystalline lens exposure dose reduction and position-matching accuracy with a reduced blade X2 aperture. The maximum reduction rate in crystalline lens exposure dose was -38.7% for the right lens and -13.2% for the left lens with an X2 of 5.0 cm. The right crystalline lens exposure dose decreased rapidly between -10.8% at 8.5 cm and -25.4% at 7.5 cm. The left crystalline lens exposure dose decreased more slowly than the right (Fig. 7 and Table 1). The distance between CBCT isocenter and RPLD was measured at the X-ray tube angles at which the primary X-ray enter the RPLD; 6.9–8.5 cm at 292–242° for the right RPLD and 7.8–8.7 cm at 292–267° for the left RPLD. In the right crystalline lens, because the exposure dose rapidly decreased the X2 aperture and the distance between CBCT isocenter and RPLD when the primary X-rays incident on the RPLD matched, we believe that X2 shielded the RPLD, resulting in a rapid decrease in the crystalline lens exposure dose. In contrast, in the left crystalline lens, primary X-rays at 292–267° were shielded by X2 but not at 118–88° because the crystalline lens was on the X1 side, resulting in a gradual decrease in the crystalline lens exposure dose. On the other hand, CBCT images with X2 set to 5.0 cm caused artifacts due to the missing imaging range; however, the amount of position

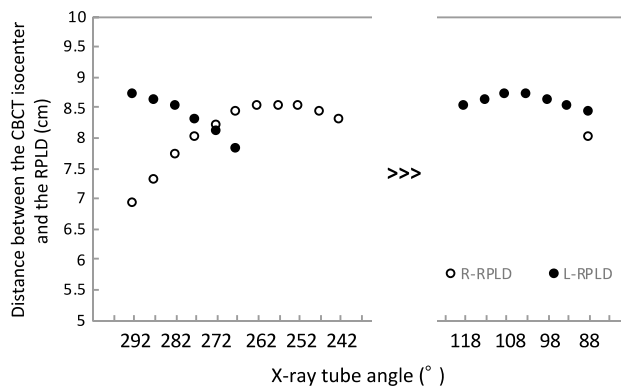
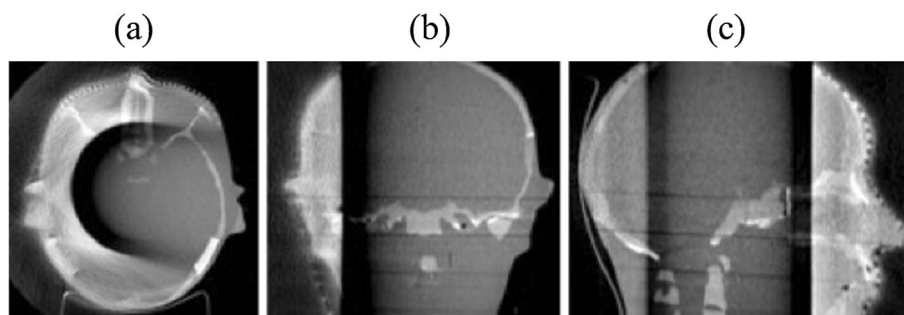


**Fig. 8** Distance between the CBCT isocenter and the RPLD at the X-ray tube angle where the primary X-rays incident on the RPLD. The white and black circles indicate the right and left crystalline lenses, respectively. To make the graphs easier to observe, X-ray tube angles (242–118°) where the X-rays do not incident on the RPLD are omitted

**Table 2** Matching accuracy in auto-matching when blade X2 aperture is set to 5.0 cm. The amount of position correction against the amount of phantom movement in the XYZ axes when X2 is set to 13.6 cm and 5.0 cm is shown. The amount of position correction is the average value of five auto-matchings

Direction of movement	Blader X2 Aperture (cm)	Amount of movement (mm)										
		-5	-4	-3	-2	-1	0	1	2	3	4	5
X axis	13.6	5	4	3	2	1	0	-1	-2	-3.4	-4	-5
	5.0	5	4.2	2.8	1	1	0	-1	-2	-4	-4	-5
Y-Axis	13.6	5	4	3	2	1	0	-1	-2	-3	-4	-5
	5.0	5	4	3	2	1	0	-1	-2	-3	-4	-5
Z-axis	13.6	5	4	3	2	1	0	-1	-2	-3	-4	-5
	5.0	5	4	3.2	2	1	0	-1	-2	-3	-4	-5

**Fig. 9** CBCT images at a blade X2 aperture of 5 cm. **a** Transverse plane, **b** coronal plane, and **c** sagittal plane



correction by auto-bone matching was within 1 mm in all movement directions. Takei et al. [22] reported that the difference in the amount of position correction by auto-bone matching was within 1 mm between CBCT with the same imaging dose as in this study and CBCT with the imaging dose reduced by half, and concluded that IGRT can be performed even on noisy images with a reduced imaging dose. A 1 mm difference is not a problem when the planning target volume (PTV) can be set sufficiently large; however, when the PTV is small, as in SRT, careful position matching is necessary. Although artifacts occurred in the X2 aperture reduced image, the bones could be recognized; therefore, we believe that manual position matching is also possible.

In clinical practice, the crystalline lens exposure dose decreases by reducing X2; however, there are concerns about the impact on the image owing to a missing imaging area. Therefore, it is necessary to set X2 to ensure a reduction in the crystalline lens exposure dose and image quality that allows position matching. To this end, we recommend measuring the distance between CBCT isocenter and right lens in Beam's Eye View at the X-ray tube angle of  $292^\circ$  during treatment planning and setting that distance to the X2 aperture. The distance between the CBCT isocenter and crystalline lens at the X-ray tube angle of  $292^\circ$  coincides with X2 aperture, where the exposure dose to the right crystalline lens decreases rapidly, and the imaging area can be secured, thus reducing both the exposure dose and ensuring image quality for position matching. However, if the CBCT isocenter is set near the crystalline lens, it is difficult to ensure image quality for position matching because X2 aperture must be extremely reduced. If the CBCT isocenter is set at

the rear of the crystalline lens (occipital lobe or cerebellum), the crystalline lens exposure dose can be reduced simply by slightly reducing X2 aperture, thus minimizing the effect on image quality. In clinical practice, when reducing the crystalline lens exposure dose by reducing X2 aperture, it is necessary to consider X2 aperture according to the CBCT isocenter in consideration of position matching. This method is useful because it can reduce the crystalline lens exposure dose using a simple technique (simply by reducing X2 aperture).

When X2 was set to the default setting (13.6 cm), the crystalline lens exposure dose was 0.84 mGy on the right and 0.82 mGy on the left, and when X2 was 5.0 cm, the dose was 0.52 mGy on the right and 0.71 mGy on the left. Based on this data, we use a clinical example to consider reducing the crystalline lens exposure dose when reducing X2 aperture. The calculated crystalline lens exposure doses in the 4 fractions SRT for the brain metastasis [23–25] are 3.36 mGy for the right and 3.28 mGy for the left at the default setting, and 2.08 mGy for the right and 2.84 mGy for the left at the 5.0 cm setting. Therefore, the exposure dose reduction is 1.28 mGy for the right and 0.44 mGy for the left. On the other hand, the calculated crystalline lens exposure doses in the 30 fractions radiotherapy for glioblastoma [26–28] are 25.2 mGy for the right and 24.6 mGy for the left at the default setting, and 15.6 mGy for the right and 21.3 mGy for the left at the 5.0 cm setting. Therefore, the exposure dose reduction is 9.6 mGy for the right and 3.3 mGy for the left. Although the crystalline lens exposure dose reduction in the SRT for brain metastases is lower than that in the radiotherapy for glioblastoma, it is important to keep the

crystalline lens exposure dose as low as possible regardless of the number of CBCT scans because the As Low As Reasonably Achievable (ALARA) principle also applies to the exposure dose in the IGRT [14]. In addition, since the severity of cataracts depends on the exposure dose, the crystalline lens exposure dose should be reduced as much as possible.

This study showed that the crystalline lens exposure dose could be reduced by reducing the blade X2 aperture. However, acceptable image quality (X2 according to the treatment position) for position matching has not been evaluated, and further studies are warranted.

## 5 Conclusion

CBCT of the head showed that the crystalline lens exposure dose could be reduced by reducing blade X2 aperture. When the CBCT isocenter was set at the center of the head, the position-matching accuracy was the same when X2 was set at 13.6 cm and 5.0 cm. Therefore, reducing the X2 aperture during CBCT imaging is a useful technique for reducing the crystalline lens exposure dose while ensuring the accuracy of position matching. When reducing X2 aperture in clinical practice, it is recommended to measure the distance from the CBCT isocenter to the right lens using Beam's Eye View at the X-ray tube angle of 292° during treatment planning and that the distance be set as X2 aperture.

**Data availability** Data sharing not applicable to this article as no datasets were generated or analyzed during the current study.

## Declarations

**Conflict of interest** The authors declare no conflicts of interest.

**Ethics approval** This study did not involve human subjects as such ethical approval was not required.

## References

1. ICRP. The 2007 Recommendations of the International Commission on Radiological Protection. ICRP Publication 103. Ann. ICRP 2007; doi: <https://doi.org/10.1016/j.icrp.2007.10.003>
2. ICRP publication 118: ICRP statement on tissue reactions and early and late effects of radiation in normal tissues and organs-threshold doses for tissue reactions in a radiation protection context. Ann. ICRP 2012. doi: <https://doi.org/10.1016/j.icrp.2012.02.001>
3. Nakashima E, Neriishi K, Minamoto A. A reanalysis of atomic-bomb cataract data, 2000–2002: a threshold analysis. Health Phys. 2006. <https://doi.org/10.1097/01.hp.0000175442.03596.63>.
4. Neriishi K, Nakashima E, Minamoto A, et al. Postoperative cataract cases among atomic bomb survivors: radiation dose response and threshold. Radiat Res. 2007. <https://doi.org/10.1667/RR0928.1>.
5. Marcus KJ, Goumnerova L, Billett AL, et al. Stereotactic radiotherapy for localized low-grade gliomas in children: final results of a prospective trial. Int J Radiat Oncol Biol Phys. 2005. <https://doi.org/10.1016/j.ijrobp.2004.06.012>.
6. Monjazeb AM, Ayala D, Jensen C, et al. A phase I dose escalation study of hypofractionated IMRT field-in-field boost for newly diagnosed glioblastoma multiforme. Int J Radiat Oncol Biol Phys. 2012. <https://doi.org/10.1016/j.ijrobp.2010.10.018>.
7. Habets EJJ, Dirven L, Wiggeraad RG, et al. Neurocognitive functioning and health-related quality of life in patients treated with stereotactic radiotherapy for brain metastases: a prospective study. Neuro Oncol. 2016. <https://doi.org/10.1093/neuonc/nov186>.
8. Hoppe BS, Stegman LD, Zelefsky MJ, et al. Treatment of nasal cavity and paranasal sinus cancer with modern radiotherapy techniques in the postoperative setting—the MSKCC experience. Int J Radiat Oncol Biol Phys. 2007. <https://doi.org/10.1016/j.ijrobp.2006.09.023>.
9. Bragga CM, Wingate K, Conway J. Clinical implications of the anisotropic analytical algorithm for IMRT treatment planning and verification. Radiother Oncol. 2008. <https://doi.org/10.1016/j.radonc.2008.01.011>.
10. Liu X, Huang E, Wang Y, et al. Dosimetric comparison of helical tomotherapy, VMAT, fixed-field IMRT and 3D-conformal radiotherapy for stage I-II nasal natural killer T-cell lymphoma. Radiat Oncol. 2017. <https://doi.org/10.1186/s13014-017-0812-1>.
11. Kan MW, Leung LH, Wong W, et al. Radiation dose from cone beam computed tomography for image-guided radiation therapy. Int J Radiat Oncol Biol Phys. 2008. <https://doi.org/10.1016/j.ijrobp.2007.08.062>.
12. Zhou L, Bai S, Zhang Y, et al. Imaging Dose, Cancer risk and cost analysis in image-guided radiotherapy of cancers. Sci Rep. 2018. <https://doi.org/10.1038/s41598-018-28431-9>.
13. Özseven A, Dirican B. Evaluation of patient organ doses from kilovoltage cone-beam CT imaging in radiation therapy. Rep Pract Oncol Radiother. 2021. <https://doi.org/10.5603/RPOR.a2021.0038>.
14. Ding GX, Alaei P, Curran B, et al. Image guidance doses delivered during radiotherapy: Quantification, management, and reduction: Report of the AAPM Therapy Physics Committee Task Group 180. Med Phys. 2018. <https://doi.org/10.1002/mp.12824>.
15. Zhang Y, Wu H, Chen Z, et al. Concomitant imaging dose and cancer risk in image guided thoracic radiation therapy. Int J Radiat Oncol Biol Phys. 2015. <https://doi.org/10.1016/j.ijrobp.2015.06.034>.
16. Ding GX, Munro P, Pawlowski J, et al. Reducing radiation exposure to patients from kV-CBCT imaging. Radiother Oncol. 2010. <https://doi.org/10.1016/j.radonc.2010.08.005>.
17. International Electrotechnical Commission. 2011. IEC 61217 Radiotherapy equipment - Coordinates movements and scales: International Electrotechnical Commission, Geneva, Switzerland
18. Seltzer SM, Hubbell JH. Tables of X-ray mass attenuation coefficients and mass absorption coefficients 1 keV to 20 MeV for elements Z=1 to 92 and 48 additional substances of dosimetric interest (NISTIR 5632). Washington, D.C.: National Institute of Standards and Technology; 1995.
19. Hsu SM, Yang HW, Yeh TC, et al. Synthesis and physical characteristics of radiophotoluminescent glass dosimeters. Radiat Meas. 2007. <https://doi.org/10.1016/j.radmeas.2007.01.053>.
20. Kim JS, Park BR, Yoo J, et al. Measurement uncertainty analysis of radiophotoluminescent glass dosimeter reader system based on GD-352M for estimation of protection quantity. Nucl Eng Technol. 2022. <https://doi.org/10.1016/j.net.2021.08.016>.
21. Trivedi G, Singh PP, Oinam AS, et al. Cone-beam computed tomography (CBCT) dose optimization technique and image

- quality assessment scoring. *J Cancer Res Ther.* 2023. [https://doi.org/10.4103/jcrt.jcrt\\_1130\\_22](https://doi.org/10.4103/jcrt.jcrt_1130_22).
22. Takei Y, Monzen H, Matsumoto K, et al. Registration accuracy with the low dose kilovoltage cone-beam CT: a phantom study. *BJR Open.* 2019. <https://doi.org/10.1259/bjro.20190028>.
  23. Kwon AK, Dibiase SJ, Wang B, et al. Hypofractionated stereotactic radiotherapy for the treatment of brain metastases. *Cancer.* 2009. <https://doi.org/10.1002/cncr.24082>.
  24. Nagai A, Shibamoto Y, Yoshida M, et al. Treatment of single or multiple brain metastases by hypofractionated stereotactic radiotherapy using helical tomotherapy. *Int J Mol Sci.* 2014. <https://doi.org/10.3390/ijms15046910>.
  25. Shiue K, Sahgal A, Lo SS. Precision radiation for brain metastases with a focus on hypofractionated stereotactic radiosurgery. *Semin Radiat Oncol.* 2023. <https://doi.org/10.1016/j.semradonc.2023.01.004>.
  26. Roa W, Brasher PMA, Bauman G, et al. Abbreviated course of radiation therapy in older patients with glioblastoma multiforme: a prospective randomized clinical trial. *J Clin Oncol.* 2004. <https://doi.org/10.1200/JCO.2004.06.082>.
  27. Minniti G, Scaringi C, Lanzetta G, et al. Standard (60 Gy) or short-course (40 Gy) irradiation plus concomitant and adjuvant temozolomide for elderly patients with glioblastoma: a propensity-matched analysis. *Int J Radiat Oncol Biol Phys.* 2015. <https://doi.org/10.1016/j.ijrobp.2014.09.013>.
  28. Mizuhata M, Takamatsu S, Shibata S, et al. Patterns of failure in glioblastoma multiforme following Standard (60 Gy) or Short course (40 Gy) radiation and concurrent temozolomide. *Jpn j radiol.* 2023. <https://doi.org/10.1007/s11604-023-01386-2>.

**Publisher's Note** Springer Nature remains neutral with regard to jurisdictional claims in published maps and institutional affiliations.

Springer Nature or its licensor (e.g. a society or other partner) holds exclusive rights to this article under a publishing agreement with the author(s) or other rightsholder(s); author self-archiving of the accepted manuscript version of this article is solely governed by the terms of such publishing agreement and applicable law.